ISSN NO. 2320-5407

Journal homepage: http://www.journalijar.com

INTERNATIONAL JOURNAL OF ADVANCED RESEARCH

RESEARCH ARTICLE

Determination of the metallicity in Elliptical Galaxy NGC 720 using Suzaku Observations

Nasser M.A[1], *Ahmed M. Abdelbar[2], M. M. Beheary[2], M. Hamday[1], and Abdelrazek M. K. SHALTOUT[2]

1. Astronomy department-National Research Institutes Of Astronomy and Geophysics (NRIAG), Egypt.

2. Department of Astronomy and Meteorology, Faculty of Science, Al-Azhar University, Nasr City, Cairo 11884, Egypt.

Manuscript Info

Manuscript History:

Received: 15 September 2015
Final Accepted: 22 October 2015
Published Online: November 2015

Key words:

Elliptical galaxy: abundance, X-rays: galaxies, individual (NGC 720), Suzaku-XISs,

Corresponding Author

Nasser.M.A

Abstract

We have analyzed the X-ray data of NGC 720 using Suzak/XISs in band 0.3-5. Kev. The extended emission in this galaxy is well described by thin thermal emission from hot gas. The detailed analysis has allowed the determination of the abundance of oxygen, silicon, sulfur and iron. In this work, the versions of APEC model 1.3.1 and 3.0.2 are applied for comparison with previous work. The APEC with atomic database (ATOMDB) provides the best fitting spectral modeling through additional emission lines. The metal abundance of O, Mg, Si, and Fe are measured within radius 3′.

INTRODUCTION

The metal abundances of stars in these galaxies give us important constraints on theoretical models of their formation. In early-type galaxies, stellar mass loss and present type Ia the metal abundance and their ratios in the ISM can provide a cumulative fossil record on the history of star formation. The stellar metallicity reflects the past activity of star formation. In addition, a longer formation time provides a higher concentration of trapped SNe Ia products to the stars (Konami et al., 2014). The stellar metallicity of the early-type galaxies has often been investigated in optical observations of their central regions using Mg and Fe absorption lines (e.g.(Thomas et al., 2005; Bedregal et al., 2008; Kuntschner et al., 2010)).

The ASCA satellite enabled us to measure the metal abundances in the ISM of early-type galaxies through spectral fitting of Fe-L lines. Since Fe in the ISM comes from stellar mass loss and SNe Ia, the Fe abundance in the ISM is expected to be a sum of the stellar metallicity and the contribution from SNe Ia, which is proportional to the ratio of SN Ia rate to stellar mass loss rate (see (Matsushita et al., 2003)). Most isolated elliptical galaxies are compact and very faint in X-rays, this leads to from very difficult to derive well constrained abundances. A very low abundance of 0.1-0.2 was reported in the early phase (Loewenstein et al., 1994), but the accuracy was not high. The diffuse X-ray emission in NGC 720 was studied previously with ROSAT and ASCA ((Buote & Canizares 1994), 1996) and is studied in detail with Chandra in a separate paper (Buote et al., 2002).

The elliptical galaxies are known to be surrounded by a large amount of X-ray emitting hot gas, as well as clusters of galaxies. The ISM temperature ranges from 0.5 to 1 keV (e.g.,(Matsumoto et al., 1997)) so that most of its emission is radiated in the soft X-ray band. However, recent spatially-resolved X-ray spectroscopies by ROSAT, ASCA, XMM/Newton, and Chandra have revealed somewhat complex temperature structures in the core region of

clusters of galaxies. Using X-ray observations, we can directly determine the metal abundances of the ISM, and constrain the stellar metallicity of the entire galaxy. We can estimate the temperature and metallicity of the hot ISM through X-ray spectra with small systematic uncertainties. With the Suzaku X-ray satellite, O, Ne, Mg and Fe abundances of elliptical galaxies NGC 720 had been studied (e.g.,(Tawara et al., 2008)), but in this paper we measure these abundance in NGC 720 by using new calibration files and new version APEC model 3.0.2, and in finally we compare our result with (Tawara et al., 2008).

The XISs detector onboard Suzaku can constrain O, Ne, and Mg abundances well because its energy resolution is better, and its background is lower than any previous X-ray CCD detector ((Koyama et al., 2007)). Most elliptical and other early-type galaxies possess a hot and diffuse interstellar medium (ISM) that extends out to several tens of kpc. Detailed analysis of the X-ray spectra of these systems, which are dominated by a wealth of characteristic emission lines, provides a robust tool to understand the metal enrichment processes in stars and interstellar gas, and possibly to constrain the supernova history of the parent galaxies.

NGC 720 is one of the nearest giant elliptical galaxies, at distance measured from surface brightness fluctuations (SBF) calibrated to Cepheids is 285 Mpc (Tonry et al., 2001) and is one X-ray-bright, relatively isolated elliptical galaxy and is classed as an E5. In this paper, we report the high spectral resolution X-ray study of the giant elliptical galaxy NGC 720, observed by the XIS detector onboard Suzaku (Mitsuda et al., 2007). NGC 720 in position (RA, Dec) in J2000.0 (28.252, -13.739) and (z = 0.005821 is taken from the NASA/IPAC extragalactic database (NED)). We describe the observation and data reduction in section 2, the spectral analysis and results in section 3, where we describe the method for estimating background and fitting spectra, and the resulting temperature and metallicity of abundance. Additionally, we discuss the abundance and temperature and the uncertainties in spectral fit. A summary and conclusion are given in section 4. Throughout this paper, we assume a distance of 28 Mpc to NGC 720 and use the Hubble constant H_o = 72 km s^{-1} Mpc^{-1}, and the abundance ratios were taken from the solar photospheric values in (Feldman 1992) in this analysis.

The Observation and Data Reduction

In figure 1, we plot counts per unit area with radius in band 0.3-5 KeV (solid red line), and doted blue line for band 5-9 KeV. The count per unit area is constant for radius large than 5′ which mean that it is save to use region 5′ - 8′ for background area. Moreover, the number counts per unit area is constant in the band 5-9 KeV that why we will use the band 0.3-5 KeV for our spectra analysis, i.e. the ISM does not emit photons above 5 KeV. NGC 720 was observed with Suzaku 2005 December 30 to 2006 January 4.

This observation was presented by (Tawara et al., 2008), the net exposure obtained was 180 ks for each XIS sensor. We can summarize the log observation of object NGC 720 in table 1.
We analyzed the public data with PROC version 2, and the data were screened with target elevation angle above the Earth rim (ELV) > (5◦), and an elevation angle above the day Earth rim (DYE ELV) > (20◦). For the 2005 observation, we extracted spectra inside 3′ centered on the X-ray peak (figure 2). We analyzed only the XIS data in this paper, although Suzaku observations were performed with both (XIS) the X-ray Imaging Spectrometer (XIS ;
(Koyama et al., 2007)) and (HXD) and the Hard X-ray Detector (HXD; (Takahashi et al., 2007)), were in operation in their normal modes. The XIS instrument consists of four sets of X-ray CCDs (XIS0, 1, 2 and 3). XIS1 is a back-illuminated (BI) sensor, while XIS0 and 2,3 are front-illuminated (FI) ones. In these observations, the instruments were operated in normal clocking mode (8 sec. per frame) with standard 5x5 and 3x3 editing mode.

The XIS response (RMF) and ancillary response (ARF) files were produced, using the latest calibration files available distributed on 14-Mar-2015, with the ftools tasks xisrmfgen and xissimarfgen respectively. We used xisrmfgen version 2012-04-21 and xissimarfgen version 2010- 11-05 to make response matrix files (RMF) and ancillary response files (ARF), respectively. The source mode of xissimarfgen was set to SKYFITS, which is appropriate for analyzing extended objects. We note that ARFs assuming a point-source, or flat-sky are almost the same within the energy range of 0.3 to 7 keV, except for normalization. To subtract the contribution of non-X-ray background (NXB), we used xisnxbgen, which generates the NXB spectrum from a dark Earth database (Tawa et al., 2008). For background region 5′ - 8′, we generated the ARF file assuming that the emission is uniform within 20′. Moreover the simulated photons number is 2000000 for each energy bin and the gtifile parameter is read from spectra file.

The Spectral Analysis and Results

Our spectral analysis was performed using XSPEC version 12.8.2p and HEAsoft version 16.1. The spectra of XIS detectors (XIS0, XIS2 and XIS3 are combined together as FI spectra and XIS1 as BI spectra) were fitted simultaneously with a model consisting of the ISM emission, unresolved discrete sources, cosmic X-ray background (CXB), and Galactic components. Here, the spectra of the NXB were subtracted. In this section we will discuss the spectral fitting and study the emission from galactic background.

The emission from galactic background

In order to study the emission from NGC 720 correctly, we have to estimate the background accurately. This consists of the instrumental non X-ray background (NXB), the cosmic X-ray background (CXB) (Boldt 1987) and the foreground Galactic X-ray emission (GXE). We estimated the NXB spectra in each analysis region using the tool "xisntebgdgen" estimates the non-X-ray background (NXB) spectrum or image of XIS, by means of the weighted sum of the night Earth observations. We estimated the CXB contribution by using a uniform-sky ARF, which is generated with "xissimarfgen"generates the Ancillary Response Files (ARFs) of the Suzaku XIS detectors through Monte-Carlo simulations for many combination of user-input, such as arbitrary X-ray emitting region and event extracting region. Finally, we estimated the GXE, using the observation by extracting spectra in the center of the field of view. We used a uniform-sky to estimate ARF response matrix as for the CXB. The GXE consists of a Local Hot Bubble (LHB) component and a Milky Way Halo (MWH) component (Hayashi et al., 2009). These have temperatures of approximately 0:08 keV and 0:2 - 0:3 keV, respectively (e.g., (Lumb et al., 2002)). We fitted the GXE spectrum with a two-temperature APEC model for galactic absorption by multiplying with wabs model and Milky Way. We apply this model for galactic background as ***wabs (powerlaw + apec) + apec*** this model meaning that the cosmic X-ray background (CXB) can be fitted well with absorbed power law (wabs*pow) and we fit foreground Galactic X-ray emission (GXE) with un absorbed APEC model, where the temperature will be a free parameter with the metal abundances fixed to one solar. We will use APEC version 1.3.1 this version was used in (Tawara et al., 2008) in previous study and using the new version APEC 3.0.2.

Figure 3 represent the best-fit result of a spectral model of the Galactic emission. The free parameters are given in table 2. These data in reduced χ^2 (= χ^2/υ , where υ is the number of degrees of freedom = number of data bins) with a fit statistics of χ^2/υ = 886.5395/775 Reduced chi squared = 1.152847 for 769 degrees of freedom this best fit for background NGC 720 in (CXB) and (GXE) in version APEC 1.3.1. We can discuss the same data in new version APEC 3.0.2 model in table 3. For the CXB component, we adopted a power-law model with a photon index Γ = 1.6 (Tawara et al., 2008). Galactic emission arises mainly from the local hot bubble (LHB) and the Milky Way halo (MWH). The temperature and normalization of the two components in the Galactic emission were left free with the metal abundance fixed to the solar level, following previous studies (e.g., (Komiyama et al., 2009);(Konami et al., 2009) ; (Hayashi et al., 2009)) CXB and MWH components, while the temperature values of the two APEC models are consistent with the typical values for the LHB and MWH.

Unresolved discrete source

Excess X-ray emission along the Galactic plane in the energy band of 2-6 keV was detected by HEAO-1 (Worrall et al., 1982) and EXOSAT (Warwick et al., 1985). For Unresolved X-ray Emission on the Galactic Plane, we added a BREMSS model, in which the temperature at 7 keV in APEC 1.3.1 and APEC 3.0.2. The bremss model describes the total spectra of discrete source in early-type galaxies well, and was successfully used for this role in previous studies (Blanton et al., 2001). This component, as well as the ISM component, was also subjected to a common absorption with fixed $N_H = 1.55 \times 10^{20}$ cm^{-2} at the Galactic value of Dickey & Lockman (1990).

The ISM component of Hot Plasma

One of the fundamental problems in abundance measurement is how to select the most appropriate gas emission model. Even though the measured abundances critically depend on the adopted emission model, X-ray spectral

fitting often does not statistically require a complex, but realistic model. In this case, investigators tend to stop as soon as the fitting returns reasonable statistics (e.g., 2 per degree of freedom 1). However, spectral fitting results (particularly the best fit Fe abundance) can be significantly different when determined, for example, by applying a single-temperature model or a multiple-temperature model. Ideally, the gas properties can be best measured by spatially resolved spectra. If they are not available, the temperature can still be measured with moderate accuracy from the integrated emission and will be close to the emission weighted average. However, the abundance cannot be measured that way, because fitting the X-ray spectra from the multi-phase gas with a single temperature model will always return a lower abundance (Morrison & McCammon 1983). Commonly used hot plasma models are MEKAL (Mewe-Kaastra-Liedahl) and APEC (Astrophysical Plasma Emission Code; (Smith et al., 2001)), since we use vAPEC model is better represent the hot plasma emission. The strongest feature in the X-ray spectra of the hot ISM is from Fe, the Fe emission features at E = 0.7-1.0 keV (or λ = 12-17A◦) originate from various ionization stages, ranging from Ne like (with 10 electrons) Fe XVII at low temperatures (kT ~5 keV) to C-like (with 6 electrons) Fe XXI in high temperatures (kT~1 keV). The Ne and Ni emission lines are also located at E~1 keV and often mixed with stronger Fe emission features. The fit is acceptable for all regions, for the central field, we analyzed the spectra extracted from annular regions of 0′-2′ as r = 5′-8′ and r = 3′ centered on NGC 720.

Spectral fitting

We fitted each XIS spectrum separately with a spectral model consisting of an absorbed bremsstrahlung emissions and fixed the column density at $N_H = 1.55 \times 10^{20}$ cm^{-2}. The vAPEC model was used for the former model, while the abundances of O, Ne, Mg, Si, Fe were free parameters, the He, C and N abundances were fixed at 1.0 solar, and the Ar and Ca abundances were tied together with the S abundance. We divided the metals into several elemental groups [(He = C = N = Al), (O, Ne, Mg), (Si, S = Ar = Ca), (Fe = Ni)] and fixed the abundance of the He = C = N group to solar. The abundances of other groups were treated as free parameters. We used the spectra from the BI (XIS1) and FI (XIS0, 2 and 3) sensors for the energy ranges of 0.3-7.0 keV and since subtracting background lines is difficult above 7.0 keV, and the ISM does not emit photons above 7.0 keV. The energy range around the Si K-edge (1.82-1.840 keV) was ignored as a result of a problem in the response matrix, since the XIS energy calibration has not been fixed in this energy band. Thus, we utilized the r = 5′-8′ region to estimate the background level, and we collected source photons in a radius smaller than 3′ where the count rate is more than 2-times larger than the background level this region is the same region in (Tawara et al., 2008). The spectra of XIS detectors (XIS0, 1,2, and 3) were fitted simultaneously with a model consisting of the ISM emission, cosmic X-ray background (CXB), and Galactic components are included as models in the spectral fit with their spectral parameters fixed, and the NXB was subtracted. We applied this model for the emission from NGC 720 ***wabs (bremss+apec+powerlaw+vapec) + apec*** this model in two components are a BREMSS model with a temperature fixed 7.0 keV (Matsushita et al., 1994)for the hard component due to low mass X-ray binaries and vAPEC model for ISM, while APEC model in version 1.3.1 and power law for background all this multiply in photo-electric absorption using Wisconsin (Morrison & McCammon 1983) cross-sections between energy 0.03-10 keV, after apply this model change version APEC version 3.0.2 this new version apply for first time and compare between (Tawara et al., 2008) and calculate the normalization. For all of the analyzed regions, the fitted energy range was 0.3-7 keV, because spectra of less than 0.3 keV is difficult to analyze due to large systematic errors, and the contribution of NXB is dominant above ~ 7 keV (Tawara et al., 2008).

Results

Table 1: The spectral parameters of (CXB and GXE background of NGC 720) at version APEC model 1.3.1.

Region	model	parameters	value
Cosmic X-ray Background (CXB)	wabs*pow	photon-index	1.56382±2.24795E-02
	=====	normalization	1.71187E-03±3.27500E-05
Galactic X-ray Emission (GXE)	APEC	kT (keV)	0.376749±6.47935E-03
Local Hot Bubble (LHB)	====	normalization	1.50964E-03±4.43685E-05
Milky Way Hallo (MWH)	APEC	kT (keV)	0.102013±4.79362E-03
	====	normalization	3.29784E-03±5.24223E-04

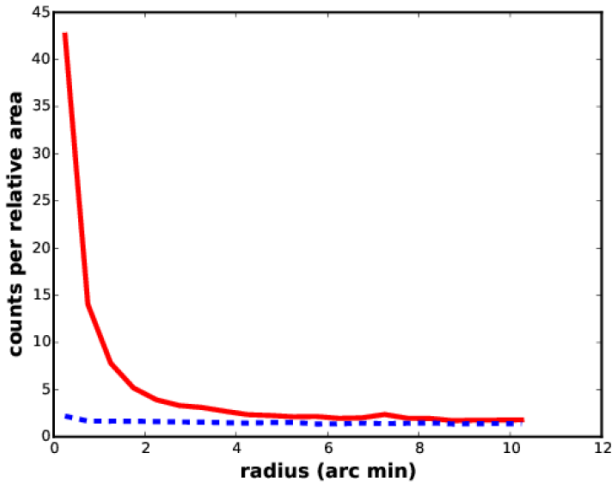

Figure 1: The plot of counts per unit area with radius, inferred from cleaned MOS1 data. The solid red line is counts per unit area in band 0.3-5 Kev but the doted blue line is in band 5-9 Kev.

Table 2: Suzaku Observation log. NGC720.

Field	Seq. No	(RA, Dec) in J2000.0	Date of Obs	Exp. time ks	Red Shift(z)
Center	800009010	28.252, 13.739	2005-12-30-2006-01-04	180	0.005821

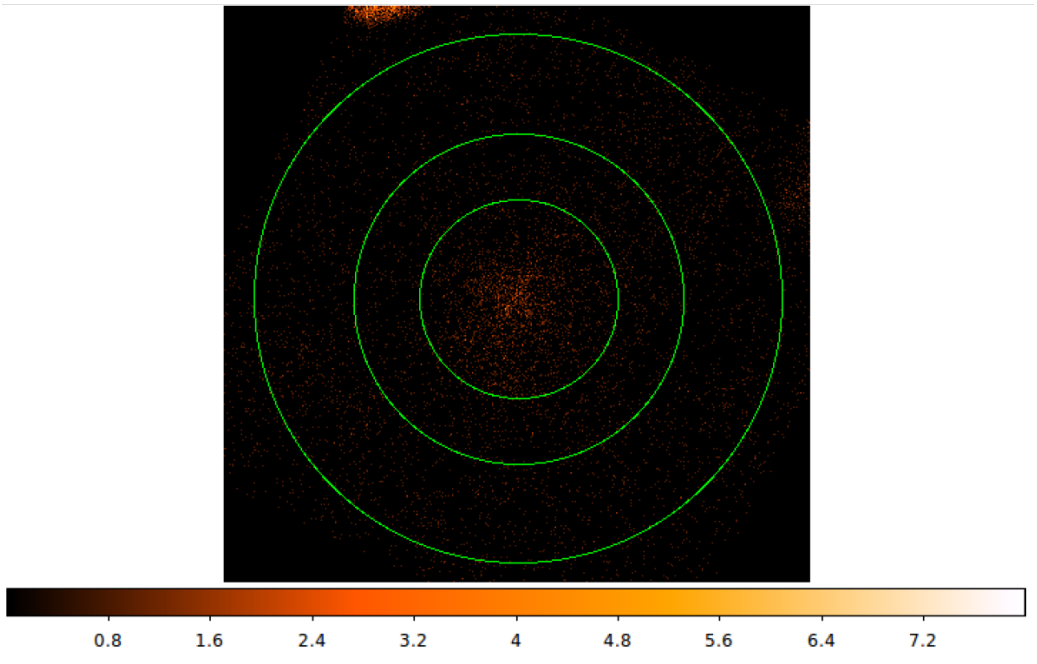

Figure 2: shows the X-ray image (0.3-5keV) of NGC 720 observation of the center region. The NXB (non- X-ray background) is subtracted, and the vignetting effects and the difference in exposure times are corrected. Boundaries of analysis regions are shown by a circle.

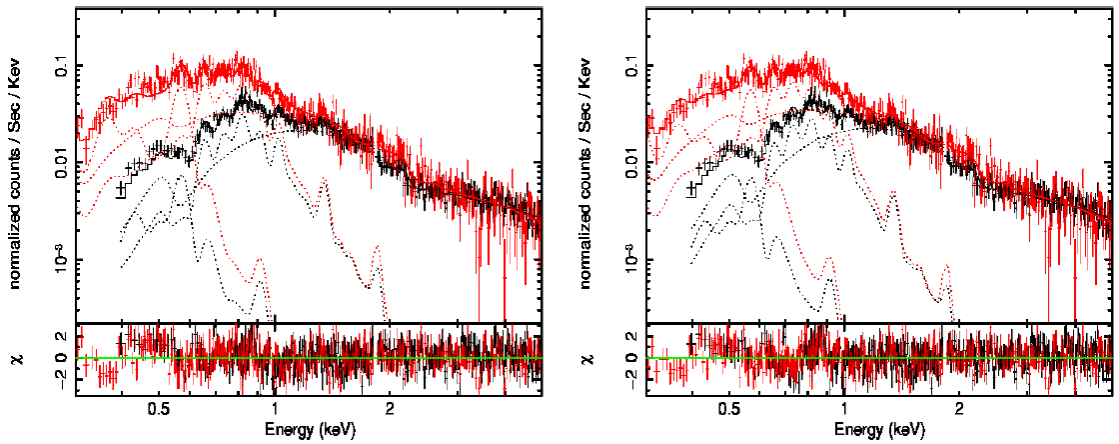

Figure 3: The best-fit result of a spectral analysis of the Galactic emission. Black and red crosses are observed spectra of FI and BI, respectively. Residuals are shown in the bottom panels (Color Online), Reduced chi-squared = 1.152847.

Table 3: The spectral parameters of (CXB and GXE background of NGC 720) at version APEC model 3.0.2.

region	Model	parameters	Value
Cosmic X-ray Background (CXB)	wabs*pow	photon-index	1.60170±2.13824E-02
	=====	normalization	1.79824E-03±3.15633E-05
Galactic X-ray Emission (GXE)	APEC	kT (keV)	0.347097±7.53317E-03
Local Hot Bubble (LHB)	====	normalization	1.25626E-03±4.14341E-05
Milky Way Hallo (MWH)	APEC	kT (keV)	0.108448±4.99271E-03
	====	normalization	2.49320E-03±3.67283E-04

The metallicity of stars in galaxies reflects the star formation history; therefore, it is an important parameter for understanding the evolution of galaxies. However, absorption-line indices that account for abundance ratios also depend on the age distribution of stars. The optical spectroscopy is a limited within the center of galaxies. Using X-ray observations, we can directly determine the metal abundances of the ISM, and constrain the stellar metallicity of the entire galaxy. The atomic data for lines at X-ray wavelengths and the structure of the hot ISM is not complex as compared with the optical spectra; therefore, we can estimate the temperature and metallicity of the hot ISM through X-ray spectra within small systematic uncertainties. By using the observations of Suzaku we will measure the abundances of O, Ne, Mg, Si and Fe of the elliptical galaxy NGC 720 with two models this is shown in table 4. According to solar abundance table of (Feldman 1992), we adopted a single-temperature vAPEC model and the abundance values (Smith et al. 2001) as the ISM thin thermal emission component. Given that the gas temperature in elliptical galaxies ranges from 0.3 keV to 1.2 keV, the strong emission lines are typically from O, Ne, Mg, Si and Fe in various ionization stages, therefore we divided the metals into several elemental groups and fixed the abundance of the He=C=N group to solar, while the abundances of other groups were treated as free parameters. Oxygen is the metallicity tracer of choice in the interstellar medium. Cosmically, its relative abundance surpasses all elements but H and He. Its relatively small depletion ((Snow & Witt 1996);(Savage & Sembach 1996)) means it is present almost entirely in the gas phase. Hot, ionized gas in the vicinity of hot stars or energetic shock waves gives rise to H II regions, planetary nebulae, or supernova remnants whose spectra usually display prominent emission lines of oxygen. This contrasts sharply with the situation for old stars, for example, where absorption features of iron (heavily depleted onto grains in the interstellar medium) are prominent in stellar spectra due to the presence of optimal temperatures. Thus, iron is usually employed as a metallicity indicator when old stars are the probes.

Table 4: Results of spectral fittings of NGC 720 with Suzaku observation in two versions APEC model

Parameters	APEC1.3.1	APEC3.0.2
kT (keV)	0.548168±3.02815E-03	0.596660±3.67260E-03
O(solar)	0.439677±4.94217E-02	0.576559±7.24991E-02
Ne(solar)	0.400472±4.85160E-02	0.657259±7.19116E-02
Mg(solar)	0.545962±5.71322E-02	0.652360±7.21135E-02
Si(solar)	0.828635±0.107403	0.838028±0.107784
Fe(solar)	0.768640±5.68241E-02	0.707014±5.67076E-02
norm vapec	5.46803E-04±3.82327E-05	4.36385E-04±3.28506E-05
norm brems	.64355E-05±2.00685E-06	9.25013E-05±2.11329E-06
	Reduced chi-squared 1.2811	degrees of freedom/PHA of bins 914/923

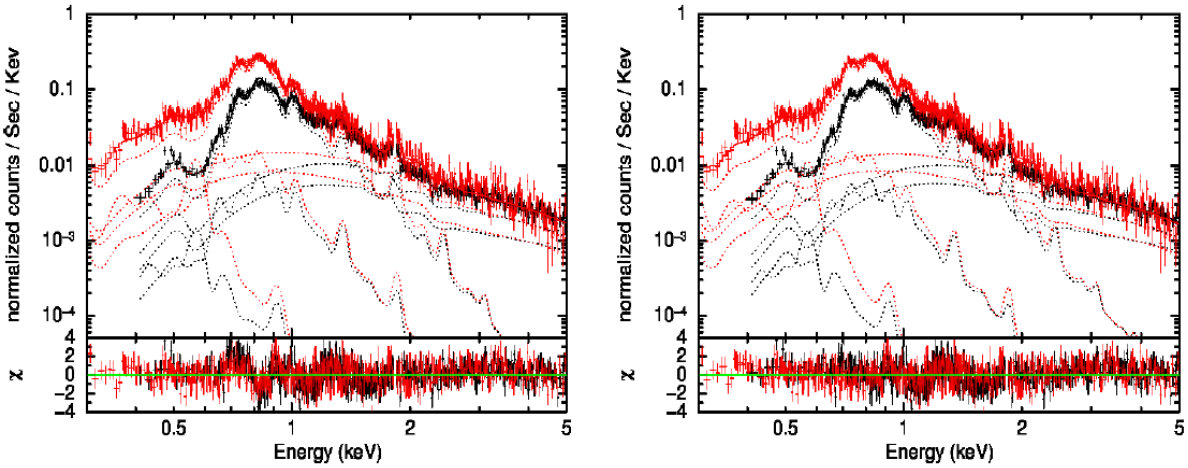

Figure 4: The spectral fitting region of NGC 720 observed by Suzaku observation. Black and red crosses are observed spectra of FI and BI, respectively. Black and red thick lines show the best-fit models to the FI and BI, of the emission plasma with using the two versions APEC for the FI and BI spectra. At the bottom panel of figure, we present residuals fit.

In figure 4 the large reduced chi-square is possibly due to the uncertainties of the Suzaku response matrices and the plasma model, and also due to the assumption of a single temperature at the center region. Analyzing with a two-temperature model as new version APEC, we could improve the reduced chi-square slightly, but this analysis gave increase in temperature. By compare our results with the results of (Tawara et al., 2008) as previous study in APEC version 1.3.1. We see about 0.2-0.4 difference between them. The temperature of high plasma about 0.55 keV this value is the same values of (Tawara et al., 2008); they measured the energy dependent effective area by comparing the temperature measured with different instruments and the normalization of the effective area by comparing the flux. In study of (Tawara et al., 2008) add the cluster of Arp 220 to improve the data in background, because this object is like in background of NGC 720, but in my data we not use this object because we used the new calibration files and new model of APEC 3.0.2.

Abundance and temperature Profiles

The temperature of the hot gas is set primarily by the depth of the potential well of the galaxy. At the temperatures found in elliptical galaxies, many of the X-ray emission is line emission due to heavy elements. Thus, X-ray spectra can be used to calculate values of the abundances, particularly the abundance of iron. It was expected that the gaseous abundances would be moderately to extremely high, depending on the supernova rate. The ISM in most elliptical is dominated by hot, kT~10^{6-7} K gas, therefore exist relation between galaxy morphology and x-ray

emission: cored galaxies this in high temperature and in ionized gas are x-ray hot gas luminous,power-law galaxies do not contain significant X-ray-emitting gas, this leads to the X-ray emission is due to the combination of thermal bremmstrahlung at high temperature and line emission from hot gas. These data include two models APEC in two version 1.3.1 for data comparison and my data in new version APEC 3.0.2, we can see about 0.2 or 0.4 differ in data but, in finally all results in this work can be observe these values is near from the abundance values of temperature of (Davis & White 1996), which calculate the value of temperature for abundance at 0.5 keV by using ROSAT satellite.

The abundance ratio

The metallicities derived from fitting thermal plasma models are driven primarily by the Fe abundance, and range from 0.1 - 0.7 solar. Since it has generally been assumed that abundances of the mass losing stars are supersolar, and since Type Ia SN are expected to further enrich the hot gas to Fe abundances of at least three times solar, X-ray abundances of elliptical galaxies are 3-30 times lower than what might naively be expected. In the halo disk the C N O abundances are almost solar, while the Ca is appears to be stable at least, and even fairly will understood. Magnesium harmonizes by being enhanced both in the bulge and in elliptical galaxies. The Ne is seems enhanced bulge, qualitatively resembling elliptical. For the metal abundance, we found that the of O, Mg, Si, Fe in NGC 720 is high, while in NGC 4382 with effective radius 4re to observe these metal abundances and the temperature is limited (Nagino & Matsushita 2010). In elliptical galaxy NGC 4382 we see low temperature and the amount of abundance by relative NGC 720 is weekly.

Most of ISM abundance ratios in elliptical galaxies are located between those of SNe Ia (present Fe abundance) and SNe II(mass loss of elements O, Mg, Ne,...). This means that the metals in the ISM are a mixture of the SNe Ia and SNe II yields. By using the results of new version APEC model 3.0.2 we can find the ratio of elements relative to the Fe see Figures 5. Figure 5 show the ratio of elements to Fe for Suzaku observation, we see the heavy element abundances in stars in the central regions of elliptical galaxies are rather high, and Type Ia supernovae may further enhance the abundances. The Si abundance is very high at atomic number 14 of Silicon element, and too from table 5 the ratio of heavy elements as Si is very higher than Fe (absolute value) this show when applying APEC 3.0.2.

Table 5: The ratio of abundance in NGC720 by relative to Fe element by using results of APEC 3.0.2 for Suzaku observations.

fixed results	ratio of abundance	Atomic number of elements
O = 0.57	O/Fe = 0.81	O = 8
Ne = 0.657	Ne/Fe = 0.938	Ne = 10
Mg = 0.652	Mg/Fe = 0.931	Mg = 12
Si = 0.83	Si/Fe = 1.18	Si = 14
Fe = 0.70		Fe = 26

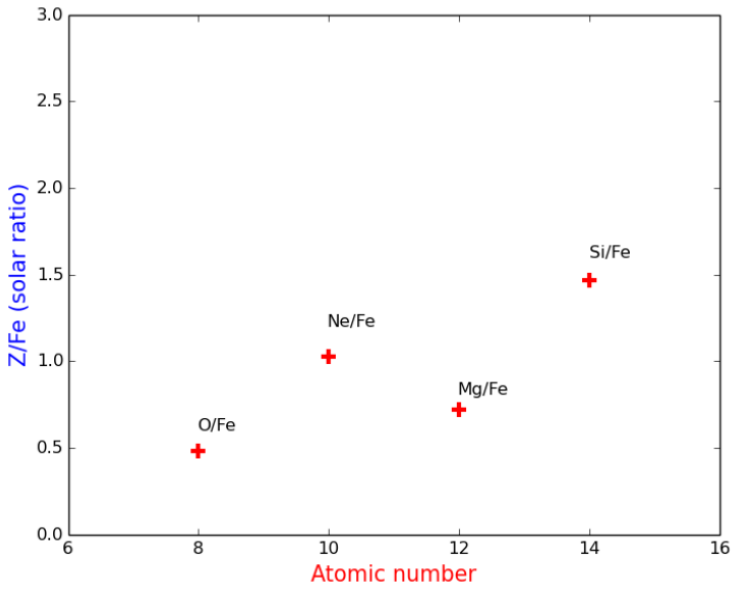

Figure 5: The relation between ratios of abundance by relative to Fe Z/Fe vs. atomic number for Suzaku observation.

Summary and Conclusion

The elliptical galaxies are the most massive and the oldest stellar systems in the universe. Analyses of their stellar spectra and their evolution with time have indicated that most of the stars formed at very high redshift. The hot X-ray-emitting ISM in these systems is the repository of the total mass loss from stellar winds, planetary nebulae, and supernovae. Accordingly, we employed the single-temperature APEC model (Smith et al. 2001) with the photoelectric absorption as a fitting model. Ideally, the metal abundances can be measured by fitting proper models to the observed X-ray spectra and the related uncertainties can be constrained by applying proper statistics.
Practically, however, there are various systematic effects and simplified assumptions which affect the results but are not easy to fully take into account. We notice from previous study as Chandra observations the morphological and thermal structures of the hot ISM in gas-rich elliptical galaxies are quite complex, because the stellar populations are old and stars are metal-rich and expect high (super-solar) abundances in the hot ISM, especially of Fe, due to SNIa enrichment. X-ray spectra of elliptical galaxies are adequately fit by models consisting of hot gas with subsolar Fe abundance and roughly solar Si-to-Fe ratio, plus a hard component from an ensemble of X-ray binaries. Elliptical galaxies tend to occur more frequently in denser environments (morphology-density relation (Dressler 1980)), and the galaxy formation occurred before a substantial number of Type Ia SNe could explode and contribute Fe. Suzaku satellite is better than Chandra and XMM Newton especially in study of abundance in elliptical galaxy. Suzaku is giving us:

- Oxygen and other abundances in galaxies and clusters, with promises of constraints on enrichment history and on SN models.
- Mg, Na are globally enhanced in large elliptical galaxy
- Good prospects for cluster temperature and mass maps to the virial radius.
- New sensitivity to any soft-excess cluster emission.

The information about elemental abundance ratios is valuable for considering the Suzaku results of the abundance X-ray faint elliptical galaxies. Here, we derived the elemental abundance ratio using Suzaku XIS data, since the Suzaku XIS data have a larger effective area and a better energy resolution in the lower energy band than the XMM-Newton EPIC CCDs and Chandra CCDs. We applied the vAPEC model to obtain an individual elemental abundance. We also modeled the Galactic absorption with WABS and the point source emission with the thermal bremsstrahlung BREMSS. The temperature of BREMSS was fixed to 7keV. The elemental abundances in the vAPEC model were divided into several groups (He=C=N, O, Ne, Mg, Si, S=Ar=Ca, Fe=Ni), and then the elemental abundances of the He=C=N group were fixed to 1 solar. The internal metallicity in the ISM within the galaxy, as suggested no information is available about the stellar metallicity in larger scales (Davies et al. 1993).

References

Bedregal, A. G., Aragón-Salamanca, A., Merrifield, M. R., & Cardiel, N. (2008). The link between the masses and central stellar populations of S0 galaxies. MNRAS, 387,660

Blanton, E. L., Sarazin, C. L., & Irwin, J. A. (2001). Diffuse Gas and Low-Mass X-Ray Binaries in the Chandra Observation of the S0 Galaxy NGC 1553 ApJ, 552, 106

Boldt, E. (1987). The cosmic X-ray background. Physics Reports, 146, 215

Buote, D. A. & Canizares, C. R. (1994). Geometrical evidence for dark matter: X-ray constraints on the mass of the elliptical galaxy NGC 720. ApJ, 427, 86

Buote, D. A., Jeltema, T. E., Canizares, C. R., & Garmire, G. P. (2002). Chandra Evidence of a Flattened, Triaxial Dark Matter Halo in the Elliptical Galaxy NGC 720, ApJ, 577, 183

Davies, R. L., Sadler, E. M., & Peletier, R. F. (1993). Line-strength gradients in elliptical galaxies, MNRAS, 262, 650

Davis, D. S. & White, III, R. E. (1996). ROSAT Temperatures and Abundances for a Complete Sample of Elliptical Galaxies, ApJ Lett., 470, L35

Dickey, J. M. & Lockman, F. J. (1990). H I in the Galaxy, ARA&A, 28, 215

Dressler, A. (1980), Galaxy morphology in rich clusters Implications for the formation and evolution of galaxies. ApJ, 236, 351

Feldman, U. (1992). Elemental abundances in the upper solar atmosphere, Physica Scripta , 46, 202

Hayashi, K., Fukazawa, Y., Tozuka, M., et al. (2009). Suzaku Observation of the Metallicity Distribution in the Elliptical Galaxy NGC 4636, Publications of the ASJ, 61, 1185

Komiyama, M., Sato, K., Nagino, R., Ohashi, T., & Matsushita, K. (2009). Suzaku Observations of Metallicity Distribution in the Intracluster Medium of the NGC 5044, Group, Publications of the ASJ,61, 337

Konami, S., Matsushita, K., Nagino, R., & Tamagawa, T. (2014). Abundance Patterns in the Interstellar Medium of Early-type Galaxies Observed with Suzaku, ApJ, 783, 8

Konami, S., Sato, K., Matsushita, K., et al. (2009). Suzaku Observation of the Metallicity in the Interstellar Medium of NGC 4258, Publications of the ASJ, 61, 941

Koyama, K., Tsunemi, H., Dotani, T., et al. (2007). X-Ray Imaging Spectrometer (XIS) on Board Suzaku, Publications of the ASJ, 59, 23

Kuntschner, H., Emsellem, E., Bacon, R., et al. (2010). The SAURON project - XVII. Stellar population analysis of the absorption line strength maps of 48 early-type galaxies, MNRAS, 408, 97

Loewenstein, M., Mushotzky, R. F., Tamura, T., et al. (1994). Discovery and implications of very low metal abundances in NGC 1404 and NGC 4374, ApJ Lett., 436, L75

Lumb, D. H., Warwick, R. S., Page, M., & De Luca, A. (2002). X-ray background measurements with XMM-Newton EPIC, A&A, 389, 93

Matsumoto, H., Koyama, K., Awaki, H., et al. (1997). X-Ray Properties of Early-Type Galaxies as Observed with ASCA, ApJ, 482, 133

Matsushita, K., Finoguenov, A., & Böhringer, H. (2003). XMM observation of M 87. II. Abundance structure of the interstellar and intergalactic medium, A&A, 401, 443

Matsushita, K., Makishima, K., Awaki, H., et al. (1994). Detections of hard X-ray emissions from bright early-type galaxies with ASCA, ApJ Lett., 436, L41

Mitsuda, K., Bautz, M., Inoue, H., et al. (2007). The X-Ray Observatory Suzaku, Publications of the ASJ, 59, 1

Morrison, R. & McCammon, D. (1983). Interstellar photoelectric absorption cross sections, 0.03-10 keV, ApJ, 270, 119

Nagino, R. & Matsushita, K. (2010). The Abundance Pattern of O, Ne, Mg, and Fe in the Interstellar Medium of S0 Galaxy NGC 4382 Observed with Suzaku, Publications of the ASJ, 62, 787

Savage, B. D. & Sembach, K. R. (1996). Interstellar Abundances from Absorption-Line Observations with the Hubble Space Telescope, ARA&A, 34, 279

Smith, R. K., Brickhouse, N. S., Liedahl, D. A., & Raymond, J. C. (2001). Collisional Plasma Models with APEC/APED: Emission-Line Diagnostics of Hydrogen-like and Helium-like Ions, ApJ Lett., 556, L91

Snow, T. P. & Witt, A. N. (1996). Revised depletions and new constraints on interstellar dust composition, in NASA Conference Publication, Vol. 3343, NASA Conference Publication, ed. M. E. Kress, A. G. G. M. Tielens, & Y. J. Pendleton, 87–91

Takahashi, T., Abe, K., Endo, M., et al. (2007). Hard X-Ray Detector (HXD) on Board Suzaku, Publications of the ASJ, 59, 35

Tawa, N., Hayashida, K., Nagai, M., et al. (2008). Reproducibility of Non-X-Ray Background for the X-Ray Imaging Spectrometer aboard Suzaku, Publications of the ASJ, 60, 11

Tawara, Y., Matsumoto, C., Tozuka, M., et al. (2008). Suzaku Observation of the Metallicity in the Hot Interstellar Medium of the Isolated Elliptical Galaxy NGC 720, Publications of the ASJ, 60, 307

Thomas, D., Maraston, C., Bender, R., & Mendes de Oliveira, C. (2005). The Epochs of Early-Type Galaxy Formation as a Function of Environment, ApJ, 621, 673

Tonry, J. L., Dressler, A., Blakeslee, J. P., et al. (2001). The SBF Survey of Galaxy Distances. IV. SBF Magnitudes, Colors, and Distances, ApJ, 546, 681

Warwick, R. S., Turner, M. J. L., Watson, M. G., & Willingale, R. (1985). The galactic ridge observed by EXOSAT, Natur, 317, 218

Worrall, D. M., Marshall, F. E., Boldt, E. A., & Swank, J. H. (1982). HEAO 1 measurements of the galactic ridge, ApJ, 255, 111